

# Modeling evapotranspiration by combining a two-source model, a leaf stomatal model, and a light-use efficiency model



Zhongmin Hu<sup>a</sup>, Sheng Gong Li<sup>a,\*</sup>, Guirui Yu<sup>a</sup>, Xiaomin Sun<sup>a</sup>, Leiming Zhang<sup>a</sup>, Shijie Han<sup>b</sup>, Yingnian Li<sup>c</sup>

<sup>a</sup> Synthesis Research Center of Chinese Ecosystem Research Network, Key Laboratory of Ecosystem Network Observation and Modeling, Institute of Geographic Sciences and Natural Resources Research, Chinese Academy of Sciences, Beijing 100101, China

<sup>b</sup> Institute of Applied Ecology, Chinese Academy of Sciences, 72 Wenhua Road, Shenyang 110016, Liaoning Province, China

<sup>c</sup> Northwest Institute of Plateau Biology, Chinese Academy of Sciences, Xining 810001, China

## ARTICLE INFO

### Article history:

Received 29 November 2012

Received in revised form 22 July 2013

Accepted 5 August 2013

Available online 12 August 2013

This manuscript was handled by Konstantine P. Georgakakos, Editor-in-Chief, with the assistance of Venkat Lakshmi, Associate Editor

### Keywords:

Evapotranspiration  
Canopy stomatal conductance  
Shuttleworth–Wallace model  
Ball–Berry model  
Remote sensing  
SWH model

## SUMMARY

Modeling and partitioning ecosystem evapotranspiration (ET) are important in predicting the responses of ecosystem water cycles to global climate change and land use. By incorporating the Ball–Berry stomatal conductance model and a light use efficiency-based gross primary productivity (GPP) model into the Shuttleworth–Wallace model, we developed a new model, SWH, for estimating ET with meteorological data and remote sensing products. Since the new model solved the problem of estimating canopy stomatal conductance, it can be used at sites equipped with meteorological observation systems around the world. Compared with eddy covariance measurements, the SWH model demonstrated satisfactory estimates of ET at a temperate forest and an alpine grassland. Eight meteorological variables and two remote sensing products (i.e., leaf area index, LAI, and enhanced vegetation index, EVI or normalized difference vegetation index, NDVI, or fraction of photosynthetically active radiation, FPAR) are required in our model. This will facilitate estimates of ET and its components, and further elucidate the mechanisms underlying their variations at regional scale. In addition, our model estimates ET and GPP simultaneously, making it convenient to address the coupling of these two key fluxes in terrestrial ecosystems.

© 2013 Elsevier B.V. All rights reserved.

## 1. Introduction

Evapotranspiration (ET) is an important process for ecosystem water cycles and energy balance, and is closely linked to ecosystem productivity (Jung et al., 2010; Oki and Kanae, 2006). It is therefore important to provide spatiotemporal information of ET across diverse ecosystems in order to predict the responses of ecosystem carbon and water cycles to changes in global climate and land use (Jung et al., 2010). Modeling of ET has a history of several decades (Li et al., 2009; Monteith, 1965; Shuttleworth and Wallace, 1985). Some process-based models have been developed or improved to estimate ET at diverse spatiotemporal scales (Bastiaansen et al., 2005; Hu et al., 2009; Kustas and Anderson, 2009; Monteith, 1965; Overgaard et al., 2006; Shuttleworth and Wallace, 1985; Vinukollu et al., 2011). Among these models, the Penman–Monteith model (P–M model, Monteith, 1965;) and the Shuttleworth–Wallace model (S–W model, Shuttleworth and Wallace, 1985) are mostly used (Anadranistakis et al., 2000; Hu et al., 2009; Iritz et al., 1999; Kato et al., 2004; Stannard, 1993; Tourula and Heikinheimo, 1998).

The S–W model is a two-source model developed from P–M to estimate plant transpiration and soil water evaporation separately. Studies indicate that the performance of S–W model is better than other ET models (including P–M model) at diverse ecosystems (Stannard, 1993; Zhang et al., 2008). However, one factor hindering the application of the S–W model is the estimation of canopy stomatal resistance. Canopy stomatal resistance is critical in modeling ET but usually regarded as a constant due to the difficulty in measurements or calculation. In our previous work, we used the Ball–Berry model (Ball et al., 1987) to estimate canopy stomatal resistance in S–W, which yielded good agreement between the ET prediction and observations at four grassland ecosystems (Hu et al., 2009). The Ball–Berry model incorporates the correlation between photosynthesis and stomatal conductance, air humidity, and ambient CO<sub>2</sub> concentrations based on observations and Cowan's theory of "maximum carbon gain and minimizing water loss" (Cowan and Farquhar, 1977). This model captures the essence of the coupling between photosynthesis and transpiration, and it implicitly covers the effects of diverse environmental factors on stomatal conductance (Leuning, 1995). Therefore it illustrates a strong predictive power and has been widely used to estimate stomatal conductance in physiological models (Leuning, 1995; Tuzet et al., 2003). In the Ball–Berry model, however, an important

\* Corresponding author. Tel./fax: +86 10 64889039.

E-mail address: [lisg@igsnrr.ac.cn](mailto:lisg@igsnrr.ac.cn) (S. Li).

variable, photosynthetic rate ( $P_n$ ), needs to be provided to estimate stomatal conductance. The gross primary productivity (GPP) calculated from eddy covariance measurement was used to replace  $P_n$  and illustrated satisfactory performance in our previous work. Therefore, as a substitute of  $P_n$ , GPP is needed in the combined S–W model and Ball–Berry model.

Eddy covariance measurements of GPP are only available at a limited number of sites. Fortunately, light use efficiency (LUE)-based GPP models have been developed and have yielded good predictions at individual sites to global scales. Example LUE-based models include CASA (Potter et al., 1993), GLO-PEM (Prince and Goward, 1995), VPM (Xiao et al., 2004), and EC-LUE (Yuan et al., 2007). NASA has also released a global GPP product, i.e., the MODIS (Moderate resolution Imaging Spectroradiometer) GPP product, which was calculated with a similar approach (Zhao et al., 2005). In terms of application, the LUE-based GPP model needs a few climate variables and remote sensing products, which are readily available globally.

In this study, our objective is to develop a new ET model through combining the S–W model, Ball–Berry model, and a LUE-based GPP model to estimate and partition ET with meteorological variables and remote sensing products. We will test the performance of the new model with *in site* measurements at a forest site and a grassland site. The main orientation of this work is that there are a large number of meteorological stations across the world, at which the meteorological variables are continuously measured. By using this rich dataset with the approach of this study, it would be possible to address the spatiotemporal variations in ET at diverse ecosystems in the world. Our work in this study might be a helpful beginning for this endeavor.

## 2. Materials and methods

### 2.1. Modeling

The S–W model describes the water vapor flows from soil to the atmosphere as being analogous to the flows of electric currents. It estimates the latent heat flux from the soil surface (i.e., soil water evaporation) and from the plant (i.e., plant transpiration) as two separate sources. Details of the model are available in Shuttleworth and Wallace (1985) and Hu et al. (2009).

Soil surface resistance  $r_{ss}$  and canopy stomatal resistance,  $r_{ac}$ , (i.e., the reverse of canopy stomatal conductance) are two critical input variables in the S–W model. In this study,  $r_{ss}$  was estimated as the function of soil water content (Lin and Sun, 1983):

$$r_{ss} = b_1 \left( \frac{SW_s}{SW} \right)^{b_2} + b_3 \quad (1)$$

where SW and  $SW_s$  are the soil water content and saturated water content in the surface soil ( $\text{m}^3 \text{m}^{-3}$ ), and  $b_1$  ( $\text{s m}^{-1}$ ),  $b_2$ ,  $b_3$  ( $\text{s m}^{-1}$ ) are empirical constants with  $b_1$  fixed as  $3.5 \text{ s m}^{-1}$  (Lin and Sun, 1983).

We estimated  $r_{ac}$  by introducing the Ball–Berry model in our study (Ball et al., 1987):

$$r_{sc} = \frac{1}{g_0 + a_1 P_n h_s / C_s} \quad (2)$$

where  $g_0$ ,  $a_1$  are empirical parameters,  $P_n$  ( $\mu\text{mol m}^2 \text{s}^{-1}$ ) is photosynthetic rate,  $h_s$  is leaf surface relative humidity, and  $C_s$  is leaf surface  $\text{CO}_2$  content (fixed as 390 ppm).

$P_n$  is a key driving variable to estimate  $r_{sc}$ . We used the gross primary productivity (GPP) estimated from the measurements of eddy covariance systems in our previous work (Hu et al., 2009). For the purpose of applications at the sites without GPP measurements, we estimated GPP with a satellite-based light use efficiency

model, whose scheme was similar to the GLO-PEM model (Prentice and Goward, 1995):

$$\text{GPP} = \varepsilon \times \text{PAR} \times \text{FPAR} \quad (3)$$

where PAR is the incident photosynthetically active radiation ( $\mu\text{mol m}^{-2} \text{s}^{-1}$ ), FPAR is the fraction of PAR being absorbed by the canopy. There are four methods being widely used to estimate FPAR: (1) estimated as the function of LAI and light extinction coefficient with Beer's law; (2) estimated as the function of NDVI (FPAR =  $1.24\text{NDVI} - 0.168$ , Sims et al., 2006), or (3) Enhance Vegetation Index, EVI (FPAR =  $1.2\text{EVI}$ , Fisher et al., 2008); and (4) the Moderate resolution Imaging Spectroradiometer (MODIS) FPAR product. In this study, we compared the performance of the four methods on estimating GPP and ET.  $\varepsilon$  is the light use efficiency ( $\mu\text{mol CO}_2 \mu\text{mol}^{-1} \text{PPFD}$ ), and is down-regulated by air temperature, soil water moisture, and vapor pressure deficit (VPD):

$$\varepsilon = \varepsilon_0 \times f(T) \times f(\text{SW}) \times f(\text{VPD}) \quad (4)$$

$$f(T) = \frac{(T - T_{\min})(T - T_{\max})}{(T - T_{\min})(T - T_{\max}) - (T - T_{\text{opt}})^2} \quad (5)$$

$$f(\text{SW}) = \frac{\text{SW} - Q_w}{Q_f - Q_w} \quad (6)$$

$$f(\text{VPD}) = \frac{\text{VPD}_{\max} - \text{VPD}}{\text{VPD}_{\max}} \quad (7)$$

where  $\varepsilon_0$  is the apparent quantum yield or maximum light use efficiency, and  $f(T)$ ,  $f(W)$  and  $f(\text{VPD})$  are the downward-regulation scalars for the effects of temperature, soil moisture and VPD on light use efficiency of vegetation, respectively.  $T_{\min}$ ,  $T_{\max}$  and  $T_{\text{opt}}$  are minimum, maximum and optimum air temperature ( $^{\circ}\text{C}$ ) for photosynthetic activity, respectively. If air temperature falls below  $T_{\min}$  or increases beyond  $T_{\max}$ ,  $f(T)$  is set to zero. In this study,  $T_{\min}$ ,  $T_{\text{opt}}$  and  $T_{\max}$  are set to 0, 20 and  $40^{\circ}\text{C}$ , respectively (Xiao et al., 2004).  $Q_w$  and  $Q_f$  are the soil water content at wilting point and field capacity, which were set to the observed maximum and minimum volumetric water content during the study period. If soil moisture increases beyond  $0.35 \text{ m}^3 \text{m}^{-3}$ ,  $f(W)$  was set to one, and if VPD falls below  $0.5 \text{ kPa}$ ,  $f(\text{VPD})$  was also set to one (Zhao et al., 2005).

For the new S–W model, which was incorporated with the Ball–Berry stomatal conductance model and the LUE-based GPP model, referred to as the SWH model hereafter, the input driving variables are Ta, RH, D, SW,  $R_n$ , G, PAR, WS, LAI, NDVI (or EVI, or FPAR), respectively. The parameters need to be optimized or estimated are  $b_2$ ,  $b_3$ ,  $a$ ,  $g_0$ ,  $k$ , and  $\varepsilon_0$ , respectively. The model time step was set as 16-day as the satellite products were calculated as 16-day composites. MODIS products, i.e., LAI/FPAR (MOD15A2) and NDVI/EVI (MOD13Q1) are the satellite products acquired from the website of Oak Ridge National Laboratory Distributed Active Archive Center (ORNL DAAC, 1 km, <http://daac.ornl.gov>). These MODIS products contain some cloud-contaminated or missing data (Hill et al., 2006). Therefore, before being input to the model, these products were processed with a software package TIMESAT3.0 (asymmetric Gaussian method was used) to exclude the noises and fill the gaps (Jönsson and Eklundh, 2004).

### 2.2. Parameterization and measurements of meteorological variables

The six parameters  $b_2$ ,  $b_3$ ,  $a$ ,  $g_0$ ,  $k$ , and  $\varepsilon_0$  were estimated through Monte Carlo simulations (details are described in Hu et al., 2009). Briefly, we performed 10,000 Monte Carlo simulations to select ten top-performance parameter sets, and the mean of the ten top-performance parameter sets was regarded as the best-fit parameter set. Using the data for calibration, we calculated the ratio of the

estimated  $E$  over ET  $\left(\frac{\sum E}{\sum ET}\right)$  after each simulation. The standard error of  $\frac{\sum E}{\sum ET}$  based on the simulations with the ten parameter sets was estimated to quantify the uncertainty on model partitioning. If the standard error was small, we would have high confidence in the accuracy of partitioning. *In situ* measuring of ET with eddy covariance systems was conducted in 2003–2006 at the two sites. We used the data of 2003 and 2004 for model calibration, and the data of 2005 and 2006 for validation.

The meteorological variables were measured with meteorological systems and were averaged over 16-day intervals.  $R_n$  was measured with a radiometer (Model CNR-1, Kipp & Zonnen, Delft, the Netherlands).  $G$  was measured at a depth of 5 cm with two flux plates (Model HFP01SC, Campbell Scientific Inc.). WS was measured with a cup anemometer (Model A100R, Vector Instrument, North Wales, UK). PAR above the canopy was measured with a quantum sensor (Model LI190SB, Licor Inc.).  $T_a$  and relative RH were measured with shielded and aspirated probes (Model HMP45C, Campbell Scientific Inc.). VPD was calculated as the difference between the saturation and actual vapor pressures at the given temperature based on the measured relative humidity and air temperature. SW was measured with a TDR probe at the depth of 5 cm at the grassland site, and 20 cm at the forest site (Model CS616, Campbell Scientific Inc.).

In order to test the accuracy of the LUE model on estimating GPP, the measurements of  $\text{CO}_2$  fluxes with eddy covariance (EC) systems at the two sites were used to calculate GPP. With the measurements, GPP was derived as the sum of net ecosystem  $\text{CO}_2$  exchange (NEE) and total ecosystem respiration ( $R_e$ ), and  $R_e$  was estimated from the relationship between nighttime NEE and soil temperature (or soil temperature and soil water content) (Falge et al., 2001). Root mean square error (RMSE) and relative error (RE) were used to quantify the difference between the model predictions and observations:

$$RMSE = \sqrt{\frac{\sum (O_i - M_i)^2}{N}} \quad (8)$$

$$RE = \frac{\sum (|O_i - M_i|/O_i)}{N} \quad (9)$$

where  $O_i$  and  $M_i$  was observed and modeled value, respectively.  $N$  was the total number of observations at one site.

### 2.3. Study sites

A temperate forest ecosystem and an alpine grassland ecosystem were selected to test the model performance. The two ecosystems are Chang–Bai–Shan mixed forest (CBS) and Gan–Cai–Tan alpine shrub-meadow (GCT), which are located around ChinaFLUX eddy covariance (EC) tower stations (Yu et al., 2006). The CBS site is located at the Forest Ecosystem Opened Research Station of Changbai Mountains, Chinese Academy of Sciences (128°6'E, 42°24'N, 738 m a.s.l.). The mean annual temperature is 3.6 °C, mean annual precipitation is 713 mm year<sup>-1</sup>. The area is covered by on average 200-year-old, multi-storied, multi-species mixed forest consisting of *Pinus koraiensis* (Korean pine), *Tilia amurensis* (Amur linden), *Acer mono* (Mono maple), *Fraxinus mandshurica* (Manchurian Ash), *Quercus mongolica* (Mongolian oak) and 135 other species. The mean canopy height is 26 m. A dense understory, consisting of multi-species broad-leaved shrub, has a height of 0.5–2 m. The peak leaf area index is about 6 m<sup>2</sup> m<sup>-2</sup>. The soil is classified as dark brown forest soil originating from volcanic ash (Zhang et al., 2006). The GCT site is located at the Haibei alpine grassland station on the Qinghai-Tibet Plateau (37°40'N, 101°20'E; 3293 m a.s.l.). The mean

air temperature is -1.7 °C and mean annual precipitation is 580 mm. The dominant species are *Potentilla fruticosa* (Bush cinquefoil), *Kobresia capillifolia*, *Kobresia humilis*, and *Saussurea sup-erba*. During the peak growing seasons, the vegetation reaches a height of about 60 cm, maximum LAI is about 3 m<sup>2</sup> m<sup>-2</sup>, and the canopy cover is 70–80%. The soil is silty clay loam with a heavy clay layer of 0.1–1.0 m in depth. The site is grazed by yaks and sheep only in the winter (Hu et al., 2008).

### 3. Results

The ET and GPP measured with the EC systems were used to optimize the parameters of the model. The parameterization results indicated that most of the six parameters were well constrained (with low standard deviations, Table 1). In addition, the standard deviations of  $\frac{\sum E}{\sum ET}$  based on the simulations with the ten top-performance parameter sets were also small at the two sites (0.15 and 0.63), implying that the model had good performance on ET partitioning.

FPAR is an important input variable for estimating GPP with the light-use efficiency model (Eq. (3)). The four popular methods of estimating FPAR were compared with regard to their estimation of GPP and ET. The results indicated that all methods yield similar seasonal dynamics of FPAR at both sites, which is consistent with the phenology of canopy development (Fig. 1). Especially at the GCT sites, the values of FPAR estimated by the different methods were quite close to each other. In comparison, the FPAR estimated from EVI were smaller in the growing seasons, and this deviation is more obvious at the CBS site than the GCT site. Except for the lower EVI-based FPAR, there was no general pattern in the magnitudes of FPAR estimated with the different methods. All methods illustrated that FPAR in the growing season at CBS was higher than at GCT, owing to the higher LAI and light extinction coefficient at the CBS.

The estimated GPP with the light-use efficiency model was generally in a good agreement with the measurements at both sites. With the different methods for estimating FPAR, the regression slope between measured and modeled GPP,  $K$ , was 0.87–1.20 at CBS and 0.97–1.28 at GCT, and the  $R^2$  was 0.91–0.95 at CBS and 0.95–0.97 at GCT (Fig. 2). By calculating the root mean square error (RMSE), we compared the performances of the four methods on estimating GPP. The results indicated that each method had different performances at the two sites (Table 2). For example, the MODIS FPAR product illustrated the best performance at the CBS site (RMSE = 1.29 g C m<sup>-2</sup> day<sup>-1</sup>), followed by the EVI method (RMSE = 1.32 g C m<sup>-2</sup> day<sup>-1</sup>), the NDVI method (RMSE = 1.45 g C m<sup>-2</sup> day<sup>-1</sup>), and the LAI method (RMSE = 1.70 g C m<sup>-2</sup> day<sup>-1</sup>). However, at the GCT site, the EVI method illustrated the best performance (RMSE = 0.35 g C m<sup>-2</sup> day<sup>-1</sup>), followed by the LAI method (RMSE = 0.37 g C m<sup>-2</sup> day<sup>-1</sup>), the MODIS FPAR method (RMSE = 0.54 g C m<sup>-2</sup> day<sup>-1</sup>), and the NDVI method (RMSE = 0.89 g C m<sup>-2</sup> day<sup>-1</sup>). It can be found from the above comparisons that the EVI method and MODIS FPAR illustrated desirable performance at both sites.

The estimated ET was also consistent with the EC measurements across all years at both sites, with the regression slope  $K$  between 0.87 to 0.94 at CBS and 0.95–1.03 at GCT, and the an  $R^2$  between 0.92 to 0.93 at the CBS site and 0.88 to 0.90 at the GCT site (Fig. 3). The use of different methods in estimating FPAR would introduce degrees of disagreement in GPP estimation, but such uncertainty was largely attenuated in ET estimation (Table 2). The result demonstrated that the four methods yield quite similar ET throughout the two validation years at both sites, with RMSE ranging from 0.35 to 0.38 mm day<sup>-1</sup> (i.e., kg H<sub>2</sub>O m<sup>-2</sup> day<sup>-1</sup>) at CBS and 0.34 or 0.35 mm day<sup>-1</sup> at GCT (except a RMSE of 0.39 with

**Table 1**

Values of the estimated parameters and the ratio of total estimated  $E$  to total estimated  $ET$  ( $\frac{\sum E}{\sum ET}$ ) at Chang–Bai–Shan temperate forest site (CBS) and Gan–Cai–Tan alpine grassland site (GCT). The values in the parenthesis are the standard deviation calculated from the simulations with the 10 top performance parameter sets.

Site and parameter	$b_2$	$b_3$	$a_1$	$g_0$	$k$	$\epsilon_0$	$\frac{\sum E}{\sum ET}$
CBS	3.1 (1.1)	884.1 (105)	13.1 (1.3)	0.01 (0.002)	0.87 (0.14)	0.056 (0.04)	0.15 (0.01)
GCT	1.7 (0.2)	170.5 (9.0)	40.5 (6.1)	0.02 (0.005)	0.39 (0.22)	0.077 (0.03)	0.63 (0.03)

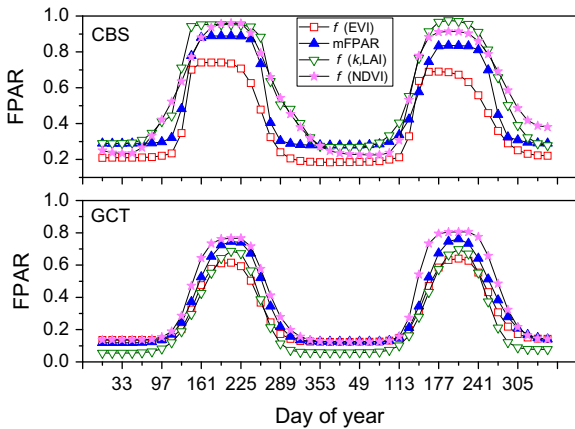


**Fig. 1.** Seasonal variations in fraction of incident photosynthetically active radiation (FPAR) derived from four methods at CBS and GCT sites.  $f(\text{EVI})$ : estimated from EVI; mFPAR: MODIS FPAR product was used;  $f(k, \text{LAI})$ : estimated with the function of light extinction coefficient ( $k$ ) and leaf area index (LAI);  $f(\text{NDVI})$ : estimated from NDVI.

the NDVI method at GCT due to the obvious higher uncertainty from GPP modeling). In comparison, the RMSE for MODIS ET (Mu et al., 2011, also from <http://daac.ornl.gov>, processed by the same method as the EVI/NDVI and LAI/FPAR products) was 0.8 and 1.1 mm day<sup>-1</sup> at CBS and GCT, respectively, illustrating poorer predictive capacity than our model, especially at the grassland site (Fig. 3).

**Table 2**

Statistical summary of model performance on predictions of gross primary productivity (GPP) and evapotranspiration (ET) comparing with observations with eddy covariance systems.  $K$  and  $R^2$  are the slope and determinant coefficient of the linear relationship between model prediction and observation with an intercept of zero. RMSE is root mean square error and RE is relative error. Four different methods were used to estimate FPAR (Eq. (3)), i.e., the function of EVI ( $f(\text{EVI})$ ), LAI ( $f(k, \text{LAI})$ ), NDVI ( $f(\text{NDVI})$ ), and the MODIS FPAR (mFPAR).

Site	Method	GPP				ET			
		$K$	$R^2$	RMSE	RE (%)	$K$	$R^2$	RMSE	RE (%)
CBS	$f(\text{EVI})$	0.87	0.91	1.32	24.4	0.87	0.93	0.38	25.2
	$f(k, \text{LAI})$	1.20	0.94	1.70	25.5	0.94	0.92	0.36	24.4
	mFPAR	1.06	0.93	1.29	27.2	0.91	0.93	0.35	24.8
	$f(\text{NDVI})$	1.17	0.95	1.45	26.1	0.93	0.92	0.35	25.2
GCT	$f(\text{EVI})$	0.97	0.97	0.35	15.0	0.95	0.90	0.35	22.5
	$f(k, \text{LAI})$	1.01	0.97	0.37	13.5	0.95	0.90	0.35	23.0
	mFPAR	1.15	0.97	0.54	17.7	0.99	0.90	0.34	22.3
	$f(\text{NDVI})$	1.28	0.95	0.89	26.0	1.03	0.88	0.39	24.2

Based on the outputs of the SWH model with the EVI method being used to estimate FPAR, the seasonal dynamics of ET,  $E$ ,  $T$ , and  $E/ET$  in 2003–2006 were quantified (Fig. 4). Consistent with our expectation,  $E/ET$  was high in non-growing seasons and low in peak growing seasons at both sites. At the CBS site,  $E/ET$  declined to near zero at the peak growing seasons due to the very dense canopy ( $\text{LAI} = 6 \text{ m}^2 \text{ m}^{-2}$ ). By contrast, the minimum  $E/ET$  at the GCT site was as high as ca. 20% with the peak LAI less than half of that at the CBS site. During the non-growing season, nearly all the water vapor flux was contributed by soil evaporation at the

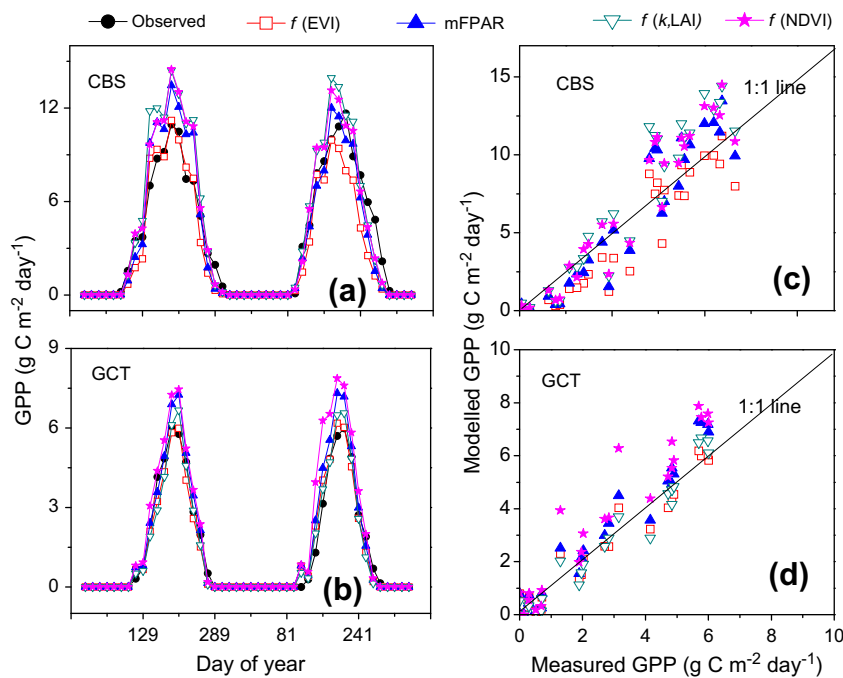


**Fig. 2.** Comparison of observed gross primary productivity (GPP) via eddy covariance system with modeled GPP via different schemes in estimating FPAR.

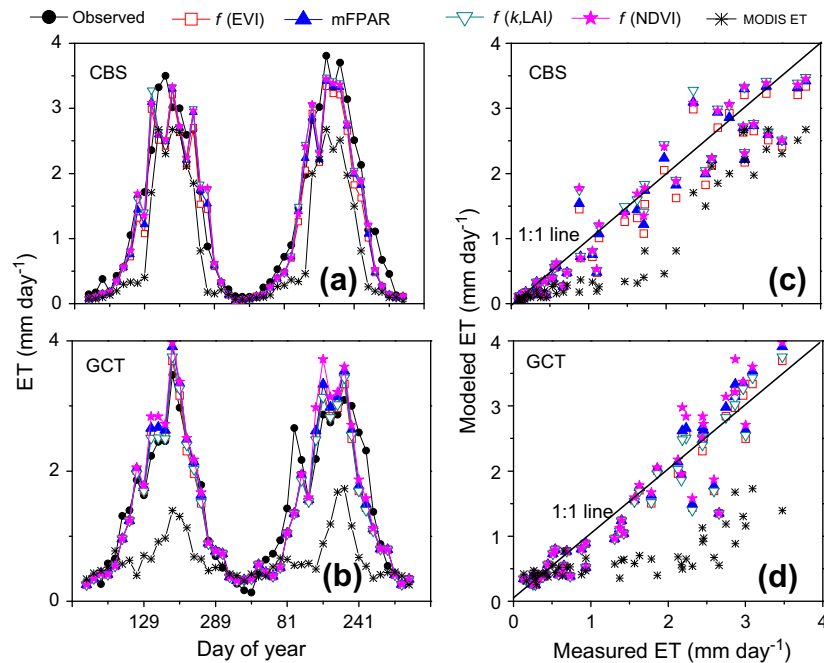


**Fig. 3.** Comparison of observed evapotranspiration (ET) via eddy covariance systems with modeled ET via different schemes in estimating FPAR, and with the MODIS ET product.

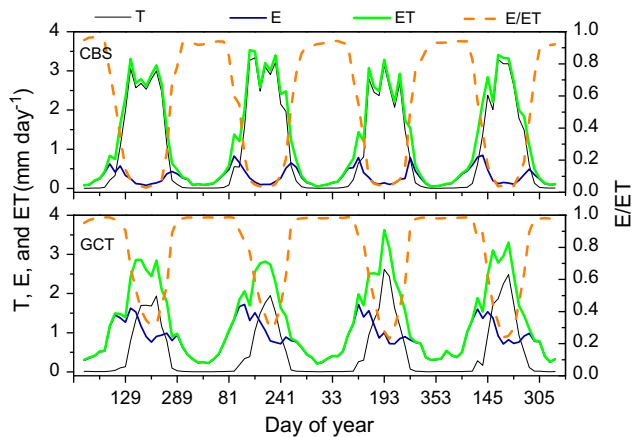


**Fig. 4.** Seasonal dynamics of ET and its components plant transpiration ( $T$ ), soil water evaporation ( $E$ ), and the ratio of  $E$  to  $ET$  ( $E/ET$ ) in 2003–2006.

GCT site. However, at the CBS site, the results illustrated that plant transpiration accounted for near 10% of  $ET$  in the non-growing season, when  $GPP$  was zero or very small. This may be due to the fact that this ecosystem is an evergreen and deciduous-mixed forest. There were still a certain amount of green leaves in the canopy in winter (with  $LAI$  ca.  $1.5 \text{ m}^2 \text{ m}^{-2}$ ), from which the water can evaporate through the stomata. In addition, the values of  $E/ET$  may have big uncertainties in non-growing seasons since the magnitudes of both  $E$  and  $T$  were very small during these periods.

#### 4. Discussion

The SWH model, in which the S–W model was incorporated with the Ball–Berry stomatal conductance model and a light use efficiency-based  $GPP$  model, demonstrated satisfactory predictive capabilities at both the forest site and the grassland site. This model illustrated a  $RMSE$  of less than  $0.4 \text{ mm day}^{-1}$  at the two sites, which is lower than most reported results. Cleugh et al. (2007) proposed a Penman–Monteith based  $ET$  model (RS-PM). A test of this

model illustrated a  $RMSE$  of ca.  $2 \text{ mm day}^{-1}$  at 19 AmeriFlux eddy covariance flux towers (Mu et al., 2007). Mu et al. (2011) updated RS-PM (i.e., the MODIS  $ET$  product), yielding a  $RMSE$  of ca.  $1 \text{ mm day}^{-1}$  at more than 46 eddy flux towers. Also, our model illustrated better performance than MODIS  $ET$  product at the two sites (Fig. 3). One may expect that the different input driving variables may be the main reason causing the different performance of the two models, i.e., tower meteorological data was used in this study but global climate data is used in MODIS  $ET$ . However, Mu's study indicates that using tower meteorological data, instead of global data, does not improve the MODIS  $ET$  product (Mu et al., 2011). We speculate that three reasons may result in better performance of SWH model over MODIS  $ET$ . First, SWH is developed from S–W model and MODIS  $ET$  is developed from P–M model. Site scale studies indicate that, due to capturing the essence of the water vapor flows within an ecosystem, S–W model illustrates better performance than PM (Stannard, 1993; Zhang et al., 2008). Second, Ball–Berry model was used in SWH to estimate canopy conductance, a key parameter in  $ET$  modeling. This may be a big contributor of the good performance of SWH model. Third, the parameters in SWH model were locally optimized but those of the MODIS  $ET$  were not. To fully compare the performance of SWH with MODIS  $ET$  or other models, global parameterization of this model is quite necessary.

The use of different schemes of estimating FPAR introduced a certain level of discrepancy in predictions of  $GPP$ . However, except for the NDVI method at the grassland site, all the schemes yielded consistent prediction of  $ET$ , suggesting that the uncertainty from FPAR is largely attenuated on  $ET$  prediction. Comparably, the EVI method and MODIS FPAR product demonstrated desirable performances on estimating  $GPP$  and  $ET$  at both sites. Six parameters were optimized with Monte-Carlo simulations in our study. We compared the estimated maximum light use efficiency,  $\epsilon_0$ , with reported values in previous studies. The  $\epsilon_0$  is estimated as  $0.056 \mu\text{mol CO}_2 \mu\text{mol}^{-1} \text{PPFD}$  at the forest site and  $0.077 \mu\text{mol CO}_2 \mu\text{mol}^{-1} \text{PPFD}$  at the grassland site. These two values are located in the middle range of  $\epsilon_0$  variations in the meta-analysis of Garbulska et al. (2010). In addition, the estimated  $\epsilon_0$  at the two

sites is also consistent with estimates from the Michaelis–Menten nonlinear model between NEE and PAR (Falge et al., 2001) at the same site ( $0.059 \mu\text{mol CO}_2 \mu\text{mol}^{-1}$  PPFD at CBS, and 0.071 at GCT, data not published).

Our model may have three merits in terms of its applications. First, it estimates ET directly by solving the problem of estimating canopy stomatal conductance via introducing the Ball–Berry model, which would largely reduce the model uncertainty from this variable. Second, relative few input variables are required in the SWH model. In our model, eight meteorological variables (i.e.,  $T_a$ , RH, VPD, SW,  $R_n$ ,  $G$ , PAR, WS) and two remote sensing products (LAI and EVI (or FPAR, NDVI)) are needed. Practically, VPD can be calculated from  $T_a$  and RH,  $G$  can be estimated as the function of  $R_n$  and NDVI (Bastiaanssen et al., 1998; Mu et al., 2011). Therefore, the number of input meteorological variables can be reduced to five in some cases, e.g., for regional applications. Third, GPP was also estimated at the same time when estimating ET with SWH model. Both ET and GPP are key fluxes in terrestrial ecosystems. These two model outputs will facilitate addressing the coupling between carbon and water processes at multiple time scales.

Notably, six parameters were optimized in the SWH model and this would be the main hindrance for its application at new sites or at regional scale. Two approaches might be used to resolve this problem. First, use empirical values from published reports. For  $b_2$  and  $b_3$  in Eq. (1), they were assigned as 2.3 and 33.5 in croplands (Lin and Sun, 1983; Wang et al., 2006). For  $a_1$  and  $g_0$  in Eq. (2), many studies have estimated these two parameters for modeling canopy stomatal conductance (Baldocchi, 1997; Collatz et al., 1991; dePury and Farquhar, 1997; Leuning, 1995). For the light extinction coefficient, an empirical value of 0.5 (or 0.6) was assigned in many biogeochemical models (e.g., Krinner et al., 2005; Sitch et al., 2003; Thornton et al., 2002). For the maximum light use efficiency ( $\epsilon_0$ , Eq. (6)), many measured values at diverse plant function types (PFTs) are available (Garbulsy et al., 2010; Kergoat et al., 2008; Yuan et al., 2007; Zhao et al., 2005). In addition, MODIS GPP product is an alternative to be used in our model without calculating FPAR and optimizing  $\epsilon_0$  (Eq. (3)). The second solution of optimizing the parameters in the SWH model is using the eddy covariance measurements around the world. There are more than 500 towers at diverse ecosystems around the world in the FLUXNET network (<http://fluxnet.ornl.gov>). With this rich dataset, PFT-specific parameter sets can be optimized with statistic methods (such as the Monte-Carlo simulations in this study), through which the model performance could be largely improved.

Note that only the two major components of evapotranspiration, i.e., soil water evaporation and plant transpiration, were considered in our model. Interception of the canopy in some ecosystems with high LAI and frequent rainfall events, may contribute a certain fraction (Lawrence et al., 2007; Mu et al., 2011; Tourula and Heikinheimo, 1998). Further study is needed to improve the algorithm by taking into account the wet canopy water evaporation.

## 5. Conclusions

In this study, by incorporating the Ball–Berry stomatal conductance model and a light use efficiency-based GPP model into the S–W model, a new two-source model, SWH, was developed for estimating and partitioning ET with meteorological variables and remote sensing products. The new model yielded satisfactory estimates of ET at a temperate forest and an alpine grassland. FPAR is a key variable in the light-use efficiency model for estimating GPP. The use of different methods to estimate FPAR, however, has very little impact on ET estimation. The SWH model estimates GPP and ET simultaneously, requiring variables and

parameters which are accessible from public databases or literature. This will facilitate addressing the variations in ET across diverse ecosystems and elucidating the mechanisms in terms of biotic and environmental conditions.

## Acknowledgements

This research was jointly funded by the National Natural Science Foundation of China (Grant No. 40971027) and the National Key Research and Development Program (Grant Nos. 2010CB833501 and 2010CB950603). The authors thank two reviewers for their helpful comments towards improving the manuscript. They also are grateful to Dr. Jared Oyler, from the Numerical Terradynamic Simulation Group (NTSG), University of Montana, to edit the manuscript for English.

## References

- Anadranistakis, M. et al., 2000. Crop water requirements model tested for crops grown in Greece. *Agric. Water Manage.* 45 (3), 297–316.
- Baldocchi, D., 1997. Measuring and modelling carbon dioxide and water vapour exchange over a temperate broad-leaved forest during the 1995 summer drought. *Plant Cell Environ.* 20 (9), 1108–1122.
- Ball, J.T., Woodrow, I.E., Berry, J.A., 1987. A model predicting stomatal conductance and its contribution to the control of photosynthesis under different environmental conditions. In: Biggins, J. (Ed.), *Progress in Photosynthesis Research*. Martinus Nijhoff, Dordrecht, pp. 221–222.
- Bastiaanssen, W.G.M. et al., 1998. A remote sensing surface energy balance algorithm for land (SEBAL) – 2. Validation. *J. Hydrol.* 213 (1–4), 213–229.
- Bastiaanssen, W.G.M. et al., 2005. SEBAL model with remotely sensed data to improve water-resources management under actual field conditions. *J. Irrig. Drain. Eng. – Asce* 131 (1), 85–93.
- Cleugh, H.A., Leuning, R., Mu, Q.Z., Running, S.W., 2007. Regional evaporation estimates from flux tower and MODIS satellite data. *Remote Sens. Environ.* 106 (3), 285–304.
- Collatz, G.J., Ball, J.T., Grivet, C., Berry, J.A., 1991. Physiological and environmental-regulation of stomatal conductance, photosynthesis and transpiration – a model that includes a laminar boundary-layer. *Agric. For. Meteorol.* 54 (2–4), 107–136.
- Cowan, I.R., Farquhar, G.D., 1977. Stomatal function in relation to leaf metabolism and environment. *Soc. Exp. Biol. Symp.* 31, 471–505.
- dePury, D.G.G., Farquhar, G.D., 1997. Simple scaling of photosynthesis from leaves to canopies without the errors of big-leaf models. *Plant Cell Environ.* 20 (5), 537–557.
- Falge, E. et al., 2001. Gap filling strategies for defensible annual sums of net ecosystem exchange. *Agric. For. Meteorol.* 107, 43–69.
- Fisher, J.B., Tu, K.P., Baldocchi, D.D., 2008. Global estimates of the land–atmosphere water flux based on monthly AVHRR and ISLSCP-II data, validated at 16 FLUXNET sites. *Rem. Sens. Environ.* 112 (3), 901–919.
- Garbulsy, M.F. et al., 2010. Patterns and controls of the variability of radiation use efficiency and primary productivity across terrestrial ecosystems. *Global Ecol. Biogeogr.* 19 (2), 253–267.
- Hill, M.J. et al., 2006. Assessment of the MODIS LAI product for Australian ecosystems. *Rem. Sens. Environ.* 101, 495–518.
- Hu, Z.M. et al., 2008. Effects of vegetation control on ecosystem water use efficiency within and among four grassland ecosystems in China. *Global Change Biol.* 14 (7), 1609–1619.
- Hu, Z.M. et al., 2009. Partitioning of evapotranspiration and its controls in four grassland ecosystems: application of a two-source model. *Agric. For. Meteorol.* 149 (9), 1410–1420.
- Iritz, Z., Lindroth, A., Heikinheimo, M., Grelle, A., Kellner, E., 1999. Test of a modified Shuttleworth–Wallace estimate of boreal forest evaporation. *Agric. For. Meteorol.* 98–9, 605–619.
- Jönsson, P., Eklundh, L., 2004. TIMESAT—a program for analyzing time-series of satellite sensor data. *Comput. Geosci.* 30 (8), 833–845.
- Jung, M. et al., 2010. Recent decline in the global land evapotranspiration trend due to limited moisture supply. *Nature* 467 (7318), 951–954.
- Kato, T., Kimura, R., Kamichika, M., 2004. Estimation of evapotranspiration, transpiration ratio and water-use efficiency from a sparse canopy using a compartment model. *Agric. Water Manage.* 65 (3), 173–191.
- Kergoat, L., Lafont, S., Arneft, A., Le Dantec, V., Saugier, B., 2008. Nitrogen controls plant canopy light-use efficiency in temperate and boreal ecosystems. *J. Geophys. Res. – Biogeosci.* 113 (G4). <http://dx.doi.org/10.1029/2007JG000676>.
- Krinner, G. et al., 2005. A dynamic global vegetation model for studies of the coupled atmosphere–biosphere system. *Global Biogeochem. Cycle* 19 (1), GB1015.
- Kustas, W., Anderson, M., 2009. Advances in thermal infrared remote sensing for land surface modeling. *Agric. For. Meteorol.* 149 (12), 2071–2081.
- Lawrence, D.M., Thornton, P.E., Oleson, K.W., Bonan, G.B., 2007. The partitioning of evapotranspiration into transpiration, soil evaporation, and canopy evaporation in a GCM: impacts on land–atmosphere interaction. *J. Hydrometeorol.* 8 (4), 862–880.

- Leuning, R., 1995. A critical-appraisal of a combined stomatal-photosynthesis model for C-3 plants. *Plant Cell Environ.* 18 (4), 339–355.
- Li, Z.L. et al., 2009. A review of current methodologies for regional evapotranspiration estimation from remotely sensed data. *Sensor* 9 (5), 3801–3853.
- Lin, J.D., Sun, S.E., 1983. Moisture and heat flow in soil and their effects on bare soil evaporation. *Water Conserv.* 7, 1–7 (in Chinese).
- Monteith, J.L., 1965. Evaporation and environment. *Soc. Exp. Biol. Symp.* 19, 205–234.
- Mu, Q., Heinsch, F.A., Zhao, M., Running, S.W., 2007. Development of a global evapotranspiration algorithm based on MODIS and global meteorology data. *Remote Sens. Environ.* 111 (4), 519–536.
- Mu, Q.Z., Zhao, M.S., Running, S.W., 2011. Improvements to a MODIS global terrestrial evapotranspiration algorithm. *Rem. Sens. Environ.* 115 (8), 1781–1800.
- Oki, T., Kanae, S., 2006. Global hydrological cycles and world water resources. *Science* 313 (5790), 1068–1072.
- Overgaard, J., Rosbjerg, D., Butts, M.B., 2006. Land-surface modelling in hydrological perspective – a review. *Biogeosciences* 3 (2), 229–241.
- Potter, C.S. et al., 1993. Terrestrial ecosystem production – a process model-based on global satellite and surface data. *Global Biogeochem. Cycle* 7 (4), 811–841.
- Prince, S.D., Goward, S.N., 1995. Global primary production: a remote sensing approach. *J. Biogeogr.* 22 (4–5), 815–835.
- Shuttleworth, W.J., Wallace, J.S., 1985. Evaporation from sparse crops – an energy combination theory. *Quart. J. Roy. Meteorol. Soc.* 111 (469), 839–855.
- Sims, D.A. et al., 2006. Parallel adjustments in vegetation greenness and ecosystem CO<sub>2</sub> exchange in response to drought in a Southern California chaparral ecosystem. *Remote Sens. Environ.* 103 (3), 289–303.
- Sitch, S. et al., 2003. Evaluation of ecosystem dynamics, plant geography and terrestrial carbon cycling in the LPJ dynamic global vegetation model. *Global Change Biol.* 9 (2), 161–185.
- Stannard, D.I., 1993. Comparison of Penman–Monteith, Shuttleworth–Wallace, and modified Priestley–Taylor evapotranspiration models for wildland vegetation in semiarid rangeland. *Water Resour. Res.* 29 (5), 1379–1392.
- Thornton, P.E. et al., 2002. Modeling and measuring the effects of disturbance history and climate on carbon and water budgets in evergreen needleleaf forests. *Agric. For. Meteorol.* 113 (1–4), 185–222.
- Tourula, T., Heikinheimo, M., 1998. Modelling evapotranspiration from a barley field over the growing season. *Agric. For. Meteorol.* 91 (3–4), 237–250.
- Tuzet, A., Perrier, A., Leuning, R., 2003. A coupled model of stomatal conductance, photosynthesis and transpiration. *Plant Cell Environ.* 26 (7), 1097–1116.
- Vinukollu, R.K., Wood, E.F., Ferguson, C.R., Fisher, J.B., 2011. Global estimates of evapotranspiration for climate studies using multi-sensor remote sensing data: Evaluation of three process-based approaches. *Rem. Sens. Environ.* 115 (3), 801–823.
- Wang, J. et al., 2006. Simulation of diurnal variations of CO<sub>2</sub>, water and heat fluxes over winter wheat with a model coupled photosynthesis and transpiration. *Agric. For. Meteorol.* 137 (3–4), 194–219.
- Xiao, X.M. et al., 2004. Modeling gross primary production of temperate deciduous broadleaf forest using satellite images and climate data. *Rem. Sens. Environ.* 91 (2), 256–270.
- Yu, G.R. et al., 2006. Overview of ChinaFLUX and evaluation of its eddy covariance measurement. *Agric. For. Meteorol.* 137 (3–4), 125–137.
- Yuan, W.P. et al., 2007. Deriving a light use efficiency model from eddy covariance flux data for predicting daily gross primary production across biomes. *Agric. For. Meteorol.* 143 (3–4), 189–207.
- Zhang, J.H., Han, S.J., Yu, G.R., 2006. Seasonal variation in carbon dioxide exchange over a 200-year-old Chinese broad-leaved Korean pine mixed forest. *Agric. For. Meteorol.* 137 (3–4), 150–165.
- Zhang, B.Z., Kang, S.Z., Li, F.S., Zhang, L., 2008. Comparison of three evapotranspiration models to Bowen ratio-energy balance method for a vineyard in an arid and desert region of northwest China. *Agric. For. Meteorol.* 148 (10), 1629–1640.
- Zhao, M.S., Heinsch, F.A., Nemani, R.R., Running, S.W., 2005. Improvements of the MODIS terrestrial gross and net primary production global data set. *Rem. Sens. Environ.* 95 (2), 164–176.